Self-Propagating High-Temperature Synthesis
Самораспространяющийся высокотемпературный синтез

UDC 621.762
https://doi.org/10.17073/1997-308X-2025-4-40-49

Research article
Научная статья

Mechanism of synthesis of ultra-high temperature Ta_4ZrC_5 carbide by thermal explosion with preliminary mechanical alloying of metals

S. G. Vadchenko, A. S. Rogachev, M. I. Alymov

Merzhanov Institute of Structural Macrokinetics and Materials Science of the Russian Academy of Sciences
8 Akademican Osip'yan Str., Chernogolovka, Moscow region 142432, Russia

vadchenko@ism.ac.ru

Abstract. Tantalum–zirconium carbide Ta_4ZrC_5 was synthesized by the method of self-propagating high-temperature synthesis (SHS) in the thermal explosion mode. The mechanism of its formation was investigated, including processes occurring during the heating of precursor mixtures to the ignition temperature, which proceed in the solid phase. The interaction of molten bimetallic Ta_4Zr particles with carbon was also studied. The initial powder mixtures were prepared in two stages. In the first stage, high-energy ball milling (HEBM) in an AGO-2 mill under an argon atmosphere was employed to carry out mechanical alloying (MA) of tantalum with zirconium, resulting in the formation of bimetallic Ta_4Zr particles representing a solid solution of zirconium in tantalum. Upon heating, ordering of the solid solution occurred, accompanied by a small exothermic effect depending on the MA duration. In the second stage, the obtained Ta_4Zr powder was mixed with carbon black and heated to the thermal explosion temperature (900–1250 °C), leading to the formation of Ta_4ZrC_5. For the first time, to study the mechanism of high-temperature interaction of Ta_4Zr bimetallic particles with carbon, the particles were deposited onto a graphite substrate and heated in vacuum at a residual pressure of 10^{-3} Pa, with the substrate temperature reaching up to 3000 °C. Depending on particle size, two modes of interaction of molten Ta_4Zr particles with the graphite substrate were observed. Particles smaller than 10 μm, due to surface tension forces, did not spread on the substrate upon melting; instead, they absorbed carbon and sank into it. Larger particles spread over the substrate, with the melt being depleted in zirconium, which more actively interacted with carbon.

Keywords: refractory compounds, high-energy ball milling (HEBM), mechanical alloying (MA), carbides

For citation: Vadchenko S.G., Rogachev A.S., Alymov M.I. Mechanism of synthesis of ultra-high temperature Ta_4ZrC_5 carbide by thermal explosion with preliminary mechanical alloying of metals. *Powder Metallurgy and Functional Coatings*. 2025;19(4):40–49. https://doi.org/10.17073/1997-308X-2025-4-40-49

Механизм синтеза ультратугоплавкого карбида Ta_4ZrC_5 в режиме теплового взрыва с предварительным механическим сплавлением металлов

С. Г. Вадченко, А. С. Рогачев, М. И. Алымов

Институт структурной макрокинетики и проблем материаловедения им. А.Г. Мержанова РАН
Россия, 142432, Московская обл., г. Черноголовка, ул. Академика Осипьяна, 8

vadchenko@ism.ac.ru

Аннотация. Методом самораспространяющегося высокотемпературного синтеза (СВС) в режиме теплового взрыва получен карбид Ta_4ZrC_5. Изучен механизм его формирования, включающий процессы в ходе нагрева смесей прекурсоров до температуры воспламенения, протекающие в твердой фазе. Исследовано взаимодействие расплавленных биметаллических частиц состава Ta_4Zr с углеродом. Исходные смеси порошков готовили в две стадии. На первой – методом высокоэнергетической механической обработки (ВЭМО) в активаторе АГО-2 в атмосфере аргона происходило механическое сплавление (МС)

смеси тантала с цирконием и формировались биметаллические частицы состава Ta_4Zr, представляющие собой твердый раствор циркония в тантале. При их нагреве происходило упорядочение твердого раствора и наблюдалось небольшое тепловыделение, зависящее от времени МС. На второй стадии полученный порошок Ta_4Zr смешивали с сажей и нагревали до температуры теплового взрыва (900–1250 °С), в результате которого образовывалось соединение Ta_4ZrC_5. Впервые для исследования механизма высокотемпературного взаимодействия биметаллических частиц Ta_4Zr с углеродом их наносили на подложку из графита и нагревали в вакууме при остаточном давлении 10^{-3} Па и температуре подложки до 3000 °С. В зависимости от размера частиц наблюдались два режима взаимодействия расплавленных частиц Ta_4Zr с подложкой из графита. Частицы размером менее 10 мкм из-за сил поверхностного натяжения при плавлении не растекались по подложке, а, растворяя в себе углерод, в нее погружались. Частицы большего размера растекались по подложке, причем расплав обеднялся цирконием, который более активно взаимодействовал с углеродом.

Ключевые слова: тугоплавкие соединения, высокоэнергетическая механическая обработка (ВЭМО), механическое сплавление (МС), карбиды

Для цитирования: Вадченко С.Г., Рогачев А.С., Алымов М.И. Механизм синтеза ультратугоплавкого карбида Ta_4ZrC_5 в режиме теплового взрыва с предварительным механическим сплавлением металлов. *Известия вузов. Порошковая металлургия и функциональные покрытия*. 2025;19(4):40–49. https://doi.org/10.17073/1997-308X-2025-4-40-49

Introduction

Binary carbides of the Ta–Zr–C system are considered promising candidates for the development of ultra-high temperature ceramics (UHTCs) [1–8]. Despite extensive research on this system, the available literature data remain contradictory, with the central question concerning the possibility of forming a single-phase carbide $Ta_{1-x}Zr_xC$. Calculation of the phase diagram of the binary Ta–Zr system has shown that below 800 °C these two metals are practically immiscible [6]. In this temperature range, a mixture of two solid solutions is formed: one based on α-zirconium with an HCP structure and the other based on tantalum with a BCC structure. The solubility of tantalum in zirconium does not exceed 2 at. %, while that of zirconium in tantalum is less than 9 at. %. A continuous series of solid solutions with a BCC structure is formed only near 1700 °C [6].

Thermodynamic investigation of the Ta–Zr–C system using the CALPHAD method led to the paradoxical conclusion that no ternary phases exist within the temperature range of 200–3600 °C [7]. This conclusion contradicts the results obtained using the CASTEP (*Cambridge Serial Total Energy Package*) code, which demonstrated the stability of $Ta_{1-x}Zr_xC$ and its structural similarity to the ultra-high temperature carbide Ta_4HfC_5 [8]. The stability of the $Ta_{1-x}Zr_xC$ phase was also demonstrated by first-principles calculations and confirmed experimentally in [9]. In particular, binary carbides with x = 0.9, 0.8, 0.6, and 0.3, synthesized by self-propagating high-temperature synthesis (SHS) from mechanically activated Ta–Zr–C mixtures and consolidated by hot pressing, showed no signs of decomposition into simple carbides after annealing at 800 °C for 40 h. Preliminary mechanical activation promotes the formation of a more homogeneous reactive mixture, enabling the synthesis of binary carbide under SHS conditions [10–12]. Along with hot pressing, a highly promising method for consolidating complex UHTCs is spark plasma sintering (SPS), in which synthesis and densification occur simultaneously [13–18]. Samples of $Ta_{1-x}Zr_xC$ UHTCs have also been produced using an original electrothermal explosion technique [19].

In studies devoted to the synthesis of $Ta_{1-x}Zr_xC$ by SHS, the primary focus has been placed on ignition and combustion parameters. The processes occurring during the preheating stage prior to ignition and the mechanism of molten metal interaction with carbon remain largely unexplored.

The aim of this work was to experimentally investigate the macrokinetic characteristics of mechanical alloying, thermal explosion, and heating of the resulting Ta_4Zr bimetallic particles, as well as the high-temperature interactions in the Ta–Zr–C system leading to the formation of $Ta_{1-x}Zr_xC$ carbide.

Materials and methods

Commercially produced powders manufactured in the Russian Federation were used in this study:

– tantalum powder, grade TaP-1 (TU 1870-258-00196109-01), 99.9 wt. % purity, particle size d = 40–63 μm;

– zirconium powder, grade PTsRK (TU 48-4-234-84), 99.6 wt. % purity, particle size d = 40–63 μm;

– carbon black, grade P804T, particle size d < 2.2 μm.

High-energy ball milling (HEBM) of tantalum and zirconium powder mixtures in a molar ratio of 4Ta:Zr was carried out in an AGO-2 planetary ball mill under an argon atmosphere. The rotational speed of the steel vials was 2220 rpm, the mass of powder mixtures was 10 g, and the mass of steel balls was 200 g. The mill-

ing time varied from 2 to 30 min. After processing and removal of the vials from the mill, their surface was heated to above 100 °C; therefore, the vials were opened only after several hours of cooling to room temperature.

As a result of HEBM, a Ta_4Zr alloy powder was obtained, a significant portion of which (up to 50 wt. %) adhered to the balls and vial walls. To grind and recover more of the alloy powder, 30 ml of hexane was added to the vials, followed by additional HEBM for 3 min. After drying, carbon black was added to the Ta_4Zr alloy powder in stoichiometric proportion to obtain Ta_4ZrC_5, and the mixture was homogenized in the AGO-2 planetary ball mill for 3–5 min.

The processes occurring during heating of Ta_4Zr alloy and during thermal explosion in the $Ta_4Zr + 5C$ and $4Ta + Zr + 5C$ mixtures were studied using the setup described in [20]. Cylindrical samples, 3 mm in diameter and up to 1.5 mm in height, were pressed from the powder mixtures and placed in a boron nitride crucible on a WRe 5/20 thermocouple rolled to a thickness of 30 μm. The crucible was positioned on a graphite strip heated by electric current. The samples were heated under constant electrical power supplied to the graphite strip, in argon at atmospheric pressure. The heating rate and maximum temperature were controlled by adjusting the electrical power. After ignition of the pellets, heating of the strip was stopped. The accuracy of temperature measurement, determined using the melting points of Zn, Al, and Cu as reference standards, was ±10 °C.

Melting and reaction of Ta_4Zr alloy powders with carbon were investigated in a VUP-5 vacuum system at a pressure of $1.3 \cdot 10^{-3}$ Pa. The powders were placed on substrates (25×5×1 mm) of fine-pored graphite (GMP) or glassy carbon (SU-2500), which were heated by direct current with a power of 1–4 kW [21]. The substrate had a fillet-like shape, allowing the narrow section to reach temperatures above 3000 °C. Before the reaction, the substrate was degassed by heating in vacuum to ~3000 °C. After cooling, bimetallic powders were deposited on its surface.

Results and discussion

Mechanical alloying

During high-energy ball milling (HEBM) of the 4Ta + Zr powder mixture, the combined effects of friction, rolling, and impacts result in mechanical alloying (MA) of tantalum and zirconium particles. Adhesion of the powder mixture to the milling balls allows observation of alloy formation in their cross-sections (Fig. 1, *a*). Initially, bimetallic layers form on the balls, which, after repeated cycles of deformation, detachment, and fracture, produce particles with a structure similar to that shown in Fig. 1, *b–d*. With increasing milling time, both the coating and the alloy particles formed upon its fracture become

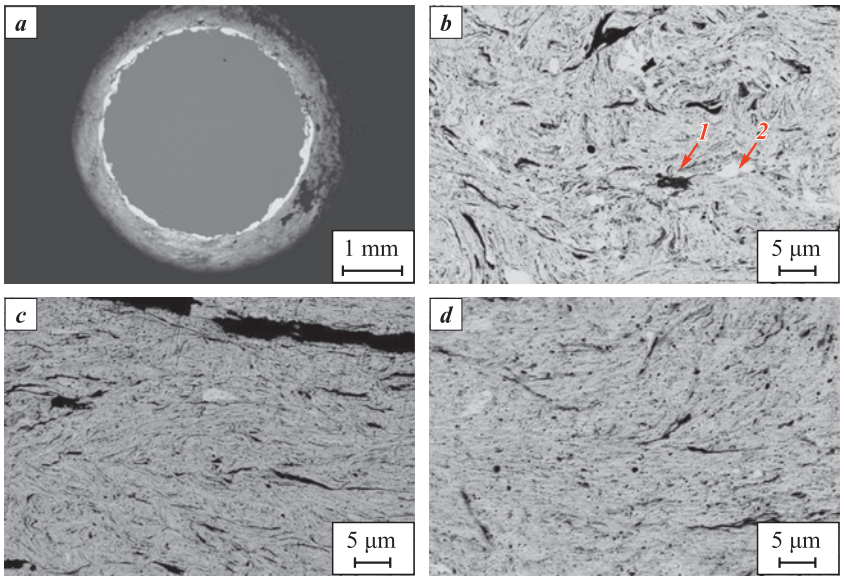

Fig. 1. Cross-section of a ball after MA of the 4Ta + Zr mixture (***a***) and fragments of the cross-section of the coating layer after HEBM for 2 (***b***), 3 (***c***) and 5 min (***d***)

1 – pore, ***2*** – tantalum particle. The light regions correspond to a higher tantalum concentration

Рис. 1. Сечение шара после МС смеси 4Ta + Zr (***a***) и фрагменты сечения слоя смеси после ВЭМО в течение 2 (***b***), 3 (***c***) и 5 мин (***d***)

1 – пора, ***2*** – частица тантала. Светлые слои содержат более высокую концентрацию тантала

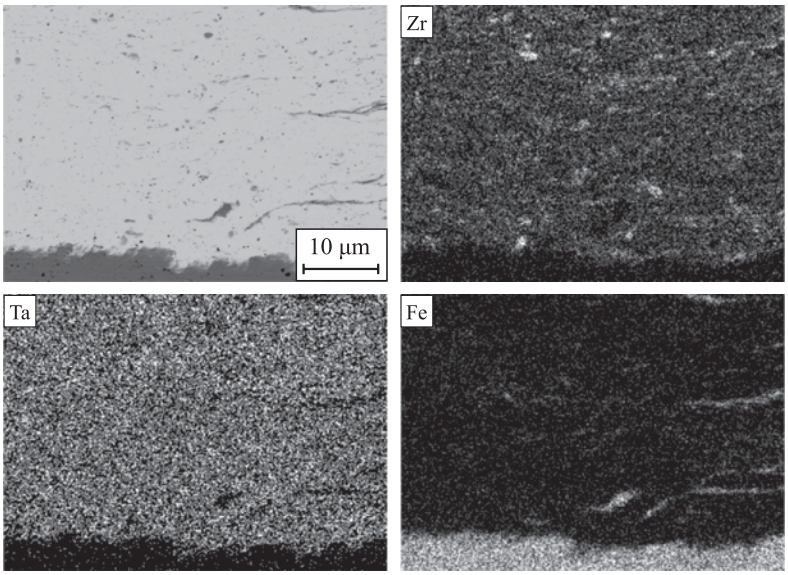

Fig. 2. Elemental distribution maps after MA of the 4Ta + Zr mixture for 10 min

Рис. 2. Карты распределения элементов после МС смеси 4Ta + Zr в течение 10 мин

more homogeneous (Fig. 2). Elemental distribution maps across particle cross-sections reveal that after 10 min of HEBM, large zirconium particles and steel fragments abraded from the milling balls are not fully broken down. Iron contamination originating from the abrasion of the steel balls and vials is an undesirable characteristic of HEBM, as it contaminates the product. The processes of particle fragmentation and iron contamination become especially pronounced during HEBM in hexane, due to the wedge action of the liquid (Rebinder effect).

At mechanical alloying times up to 5 min, complete homogenization of the alloy was not achieved; therefore, the duration was increased to 10–30 min. However, even in this case, the elemental distribution remained insufficiently uniform (see Fig. 2). Further prolongation of milling time led to significant contamination of the Ta_4Zr alloy with iron, and thus the MA time was limited to 30 min.

Results of *X*-ray diffraction analysis of the bimetallic powders

Fig. 3 shows the diffraction patterns of powders at different stages of mechanical alloying. The zirconium powder used contains some zirconium hydride, originating from the hydride–calcium reduction process by which it was produced. During MA, zirconium hydride decomposes with the release of hydrogen, and its diffraction peaks, along with those of zirconium, disappear after only 3 min of MA. This disappearance may be associated both with the refinement of zirconium crystallites and with its dissolution in tantalum.

As shown in Fig. 2, complete dissolution of zirconium does not occur even after 10 min of milling, and moreover, the mutual solubility of Zr and Ta is quite limited [6]. Therefore, the most likely reason for the disappearance of the peaks is intensive plastic deformation of zirconium, which results in crystallite refinement (reduction of coherent scattering domain size) and peak broadening. After 30 min of MA, the dif-

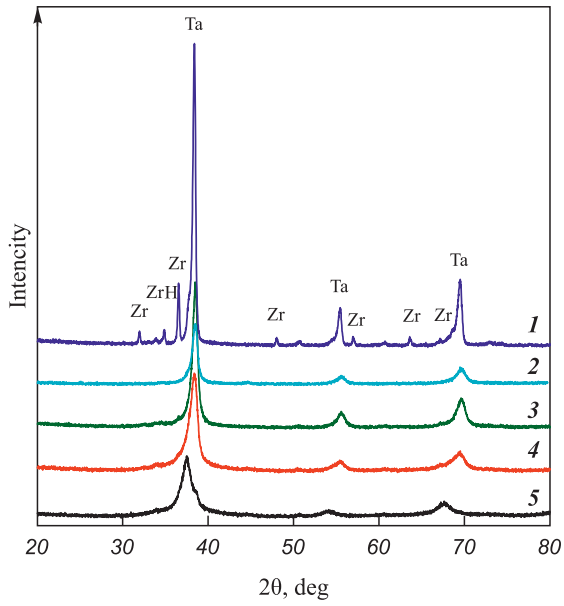

Fig. 3. XRD patterns of powders after different durations of MA

τ_{MA}, min: 0 (***1***), 3 (***2***), 10 (***3***), 20 (***4***) and 30 (***5***)

Рис. 3. Дифрактограммы порошков после различной длительности МС

$\tau_{МС}$, мин: 0 (***1***), 3 (***2***), 10 (***3***), 20 (***4***) и 30 (***5***)

fraction pattern exhibits three strongly broadened peaks characteristic of the BCC structure. The asymmetric shape of the most intense peak suggests the presence of two phases with closely spaced interplanar distances. Such a diffraction pattern may indicate the coexistence of two BCC solid solutions based on Ta.

Heating of bimetallic powders and ignition of their mixtures with carbon black

Fig. 4 shows the thermograms of primary and repeated heating of samples prepared from the initial 4Ta + Zr mixtures (curves *1a* and *1b*), Ta_4Zr bimetallic particles obtained by MA for 10 and 30 min (curves *2a*, *2b* and *3a*, *3b*, respectively), and the Ta_4Zr + 5C mixture (curves *4a*, *4b*). The inflections in the thermograms in the temperature range of 700–900 °C (curve *3*) are associated with the α → β phase transition in zirconium. Tantalum lowers the transition temperature from 863 to 800–785 °C [22; 23]. According to the phase diagram of the Zr–Fe system, dissolution of more than 4 at. % Fe in tantalum also reduces the α → β transition temperature in zirconium to 785 °C [22]. Increasing the MA time to 30 min leads to a clearer manifestation of this phase transition during powder heating. Above the phase transition temperature, an exothermic effect is observed. Heat release is proportional to the area under the Δ*t* curve, which represents the temperature difference between the primary and repeated heating of the mixtures (curves *1c–4c*). The exothermic effect increases with milling time and is most likely caused by the interaction of Ta_4Zr alloy with the abraded iron. During ignition and combustion, however, this reaction contributes only a small fraction of the heat release. For example, the enthalpy of formation of Zr_3Fe ($\Delta H(298.15) = -13.51$ kJ/mol) [6] is an order of magnitude smaller than that for the carbides ZrC ($\Delta H(298.15) = -207.1$ kJ/mol) and TaC ($\Delta H(298.15) = -141.8$ kJ/mol) [24]. This is confirmed by the heating curves of the Ta_4Zr + 5C mixture (see Fig. 4, curves *4a*, *4b*, *4c*).

Fig. 5 presents the results of studying the effect of heating and thermal explosion on the phase composition of powders. Curves *1* and *2* correspond to a BCC solid solution, while curve *3* represents the Ta_4ZrC_5 compound with an FCC structure. During heating of Ta_4Zr + 5C mixtures to the ignition temperature, ordering of the alloy structure occurs. This is evident from the reduced peak broadening and peak shifts in the diffraction pattern of Ta_4Zr bimetallic particles after short-term heating in argon (curve *2* in Fig. 5). Their reaction with carbon leads to the formation of an alloy close in composition to Ta_4ZrC_5, although in some experiments traces of Ta and its carbide Ta_2C were observed at the background level in the diffraction patterns. This can be attributed to incomplete homogeni-

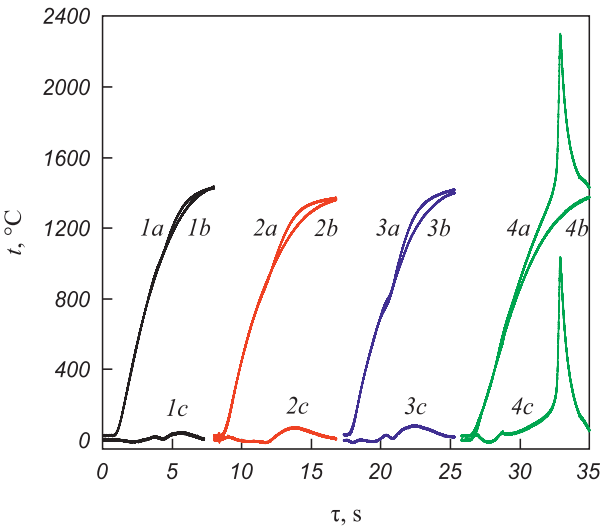

Fig. 4. Thermograms of heating of the initial 4Ta + Zr mixture (***1a***), Ta_4Zr bimetallic particles after 10 min of MA (***2a***) and 30 min of MA (***3a***), and the Ta_4Zr + 5C mixture (***4a***)
1b–4b – repeated heating; ***1c–4c*** – temperature difference (Δ*t*)

Рис. 4. Термограммы нагрева исходной смеси 4Ta + Zr (***1a***), биметаллических частиц Ta_4Zr после 10 мин МС (***2a***) и 30 мин МС (***3a***), а также смеси Ta_4Zr + 5C (***4a***)
1b–4b – повторный нагрев; ***1c–4c*** – разность температур (Δ*t*)

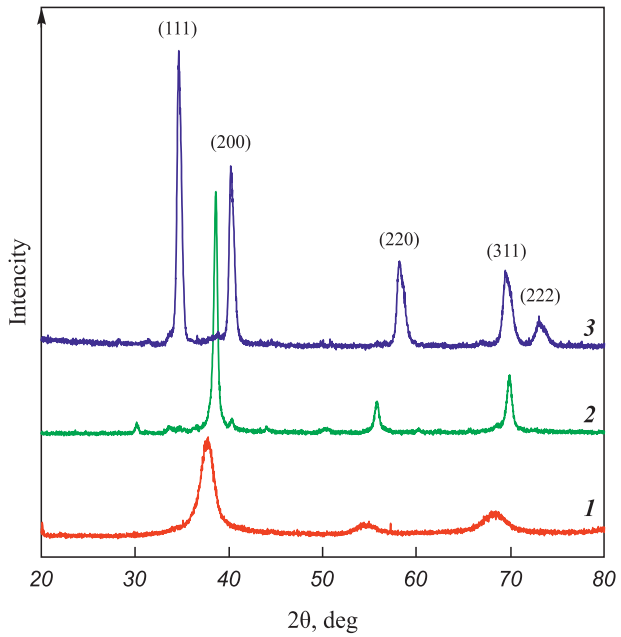

Fig. 5. XRD patterns of bimetallic powder after 30 min of MA (***1***), heating to 1400 °C for 10 s (***2***), and thermal explosion products (***3***)

Рис. 5. Дифрактограммы биметаллического порошка после 30 мин МС (***1***), нагрева до 1400 °C в течение 10 с (***2***) и продуктов теплового взрыва (***3***)

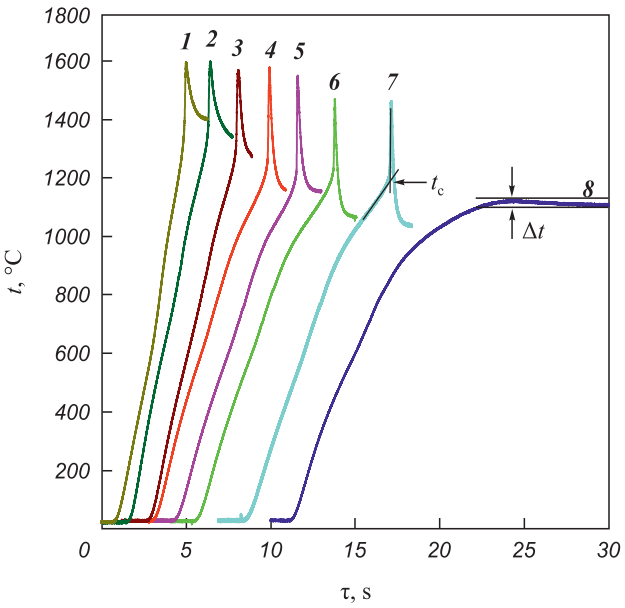

Fig. 6. Thermograms of ignition of Ta_4Zr + 5C mixtures at different average initial heating rates

v, °C/s: 277 (***1***), 275 (***2***), 260 (***3***), 205 (***4***), 195 (***5***), 190 (***6***), 185 (***7***), 180 (***8***)

Рис. 6. Термограммы воспламенения образцов из смеси Ta_4Zr + 5C при изменении средней начальной скорости нагрева

v, °C/c: 277 (***1***), 275 (***2***), 260 (***3***), 205 (***4***), 195 (***5***), 190 (***6***), 185 (***7***), 180 (***8***)

zation of the Ta_4Zr alloy at HEBM times shorter than 60 min.

Fig. 6 shows the thermograms of Ta_4Zr bimetallic particles (τ_{MC} = 5 min) mixed with carbon black and heated at different heating rates (*v*). Below 1100 °C, heating does not lead to ignition (Fig. 6, curve *8*). The critical ignition temperature (t_c) corresponds to the intersection of tangents drawn to the heating section of the sample and to the steep temperature rise. The value of tc depends on the duration of MA and the mixing time of bimetallic powders with carbon black, and may vary within 900–1250 °C. With increasing heating rate, the ignition temperature t_c also increases (Fig. 7).

Experimental results show that the ignition temperature of the mixture is significantly lower than the melting points of zirconium (1852 °C) and Ta_4Zr alloy (1855–2600 °C, depending on the degree of homogeneity) [14]. Thermodynamic calculations for the ternary system [7] also indicate that a liquid phase appears only above 1800 °C. The heating of Ta_4Zr + 5C powder mixtures observed in the 900–1100 °C range, followed by their ignition, demonstrates that the reaction initiates in the solid state. The calculated adiabatic combustion temperatures using the Thermo software [25] for the reaction 4Ta + Zr + 5C = 4TaC + ZrC are 2640 and 3180 °C at initial temperatures of 25 and 900 °C,

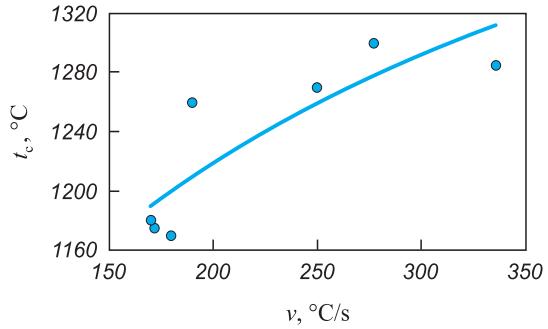

Fig. 7. Dependence of the critical ignition temperature of Ta_4Zr + 5C 5C mixtures on the heating rate

Рис. 7. Зависимость критической температуры воспламенения смесей Ta_4Zr + 5C от скорости нагрева образцов

respectively. Thus, during thermal explosion and in the combustion wave, the melting point of the bimetallic particles is reached, and the reaction proceeds via mass transport through the liquid phase.

X-ray diffraction analysis of the thermal explosion products shows the formation of a single-phase double carbide with a face-centered cubic (FCC) structure (curve *3* in Fig. 5).

High-temperature interaction of Ta_4Zr melt with carbon

The study of high-temperature reaction mechanisms is complicated by the rapid processes occurring in the combustion wave. To investigate the interaction of Ta_4Zr melt with carbon, model experiments were conducted. In these, Ta_4Zr and Ta particles were placed on graphite or glassy carbon substrates, heated to the melting point of tantalum, and held for 10–30 s. The melting of Ta (99.9 % purity, melting point 2996 °C) served as a reference for estimating substrate temperature. Energy-dispersive *X*-ray analysis showed that iron impurities present in the initial particles were absent after heating, explained by their evaporation.

The interaction of particles with the substrate depends on particle size. Small particles (d < 10 μm) did not spread under the action of surface tension forces but instead dissolved carbon and sank into the substrate (Fig. 8). This behavior is governed by the ratio between the spreading time (τ_s) and the carburization time (τ_d). For small particles, $\tau_s > \tau_d$, for large particles, $\tau_s < \tau_d$. The critical spreading time is determined by the relation $\tau_s \sim R^2/D$, where R is particle radius and D is the diffusion coefficient of carbon in the melt [26].

Melting begins at the contact point between the particle and the hot substrate. Therefore, during melting and spreading of particles larger than 10 μm, the reac-

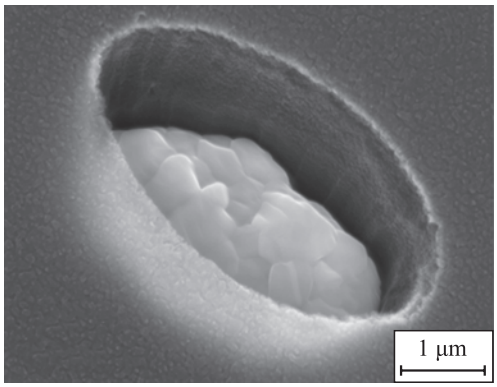

Fig. 8. Photograph of a Ta_4Zr particle that penetrated into a glassy carbon substrate upon melting

Рис. 8. Фотография частицы Ta_4Zr, погрузившейся при расплавлении в подложку из стеклоуглерода

tion initiates in the central region of the contact spot, producing a crater-like ring structure (Fig. 9).

The resulting droplets typically move along the substrate surface, leaving a trace. A characteristic feature of these structures is a reduced zirconium concentration on the surface of the spread droplet and an increased zirconium concentration in the imprint. This structure is most likely associated with the higher diffusivity of zirconium atoms in the melt and their strong affinity for carbon. In some cases, nearly all zirconium diffuses into the substrate (Fig. 10). In such cases, regions with zirconium concentrations close to the initial composition coexist with zirconium-depleted regions, which differ significantly in structure. The crater edges also exhibit high carbon content.

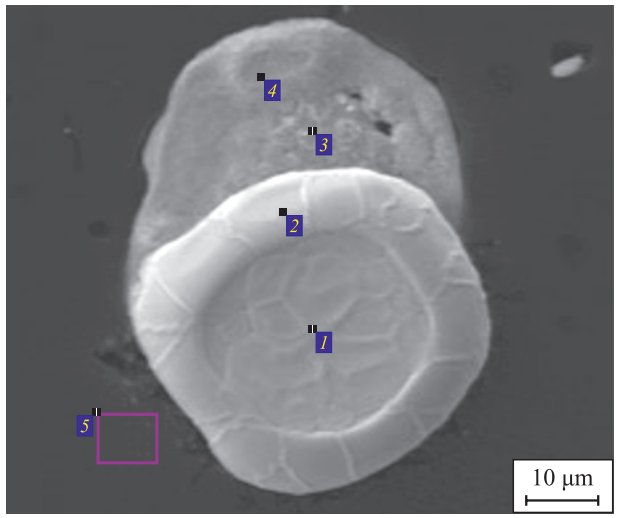

Spectrum	Content, at. %			
	C	Zr	Ta	Σ
1	9.6	3.3	87.1	100.0
2	35.7	1.7	62.6	100.0
3	15.6	16.6	67.8	100.0
4	11.3	10.4	78.3	100.0
5	98.1	1.2	0.7	100.0

Fig. 9. Photograph of a molten Ta_4Zr particle and results of its elemental analysis

Рис. 9. Фотография расплавленной частицы Ta_4Zr и результаты ее элементного анализа

Conclusions

An experimental study was conducted on the formation of the ultra-high temperature carbide Ta_4ZrC_5 by mechanical alloying in a planetary ball mill, fol-

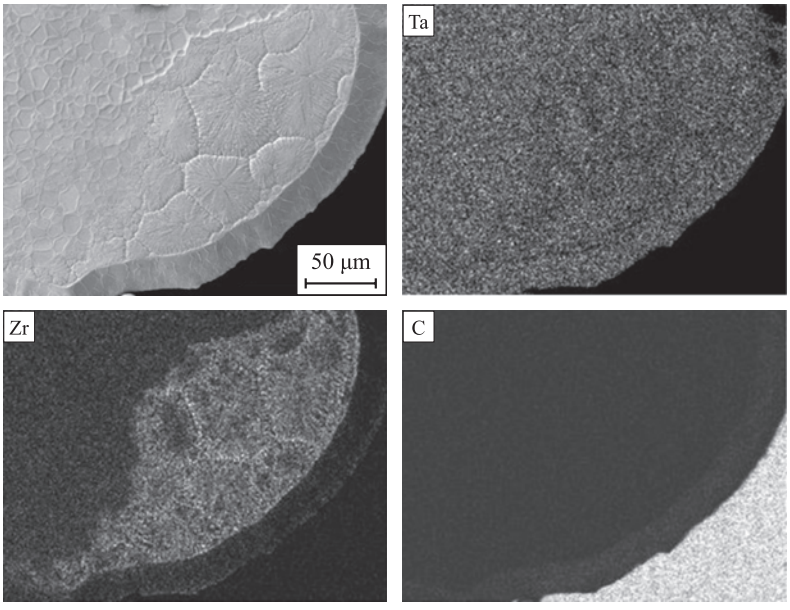

Fig. 10. Elemental distribution map of a molten particle

Рис. 10. Карты распределения элементов в расплавленной частице

lowed by synthesis in the thermal explosion mode. Model experiments simulating the processes of ignition and combustion in the high-temperature zone were also performed. The data obtained on the formation of bimetallic particles, ignition of their mixtures with carbon black, and high-temperature interaction with carbon provide new insights into the synthesis mechanism of ultra-high temperature carbides and their ceramic materials for high-temperature applications. The following conclusions can be drawn.

1. High-energy ball milling of 4Ta + Zr powder mixtures in a planetary mill yields BCC solid solutions that serve as initial reactants for subsequent synthesis. The mechanically alloyed powder consists of bimetallic particles with a characteristic layered ("compositional") structure.

2. Mixtures of bimetallic powders with carbon black undergo self-ignition upon heating in argon at 900–1250 °C, depending on heating conditions. Since these temperatures are below the melting point of the bimetallic particles, the self-sustaining reaction is initiated by solid-phase interaction.

3. As a result of the exothermic reaction of the bimetallic particles with carbon, the temperature rapidly increases beyond the melting point of the metals. The final product is formed through the interaction of the metallic melt with carbon.

4. The product of synthesis in the thermal explosion mode is the ultra-high temperature carbide Ta_4ZrC_5.

5. Model high-temperature experiments in the "molten Ta_4Zr bimetallic particles–carbon" system revealed two size-dependent interaction mechanisms: large particles spread across the carbon substrate surface with preferential zirconium diffusion into the substrate, whereas small particles predominantly absorbed carbon.

References / Список литературы

1. Andrievskii R.A., Strel'nikova N.S., Poltoratskii N.I., Kharkhardin E.D., Smirnov V.S. Melting point in systems ZrC–HfC, TaC–ZrC, TaC–HfC. *Powder Metallurgy and Metal Ceramics*.1967;(6):65–67. https://doi.org/10.1007/BF00773385
2. Gusev A.I. Phase diagrams of the pseudo-binary TiC–NbC, TiC–TaC, ZrC–NbC, ZrC–TaC, and HfC–TaC carbide systems. *Russian Journal of Physical Chemistry A*. 1985;59:336–340.

   Гусев А.И. Диаграммы состояния псевдобинарных карбидных систем TiC–NbC, TiC–TaC, ZrC–NbC, ZrC–TaC и HfC–TaC. *Журнал физической химии*. 1985; 59(3):579–584.
3. Fan Z., Zhilin T., Bin L. Research progress on carbide ultra-high temperature ceramic anti-ablation coatings for thermal protection system. *Journal of Inorganic Materials*. 2025; 40(1):1–16. https://doi.org/10.15541/jim20240317
4. Farhadizadeh A., Ghomi H. Mechanical, structural, and thermodynamic properties of TaC–ZrC ultra-high temperature ceramics using first principle methods. *Materials Research Express*. 2020;7(3):1-10. https://doi.org/10.1088/2053-1591/ab79d2
5. Wang Y., Wen B., Jiao X., Li Y., Chen L., Wang Y., Dai F.-Z.. The highest melting point material: Searched by Bayesian global optimization with deep potential molecular dynamics. *Journal of Advanced Ceramics*. 2023;12(4):803–814. https://doi.org/10.26599/JAC.2023.9220721
6. Guillermet A.F. Phase diagram and thermochemical properties of the Zr–Ta system. An assessment based on Gibbs energy modeling. *Journal of Alloys and Compounds*. 1995;226(1–2):174–184. https://doi.org/10.1016/0925-8388(95)01582-5
7. Zhou P., Peng Y., Du Y., Wang S., Wen G., Xie W., Chang K. A thermodynamic description of the C–Ta–Zr system. *International Journal of Refractory Metals and Hard Materials*. 2013;41:408–415. https://doi.org/10.1016/j.ijrmhm.2013.05.015
8. Zhang S., Liu S., Yan D., Yu Q., Ren H., Yu B., Li D. Structural stability, hardness, fracture toughness and melting points of $Ta_{1-x}Hf_xC$ and $Ta_{1-x}Zr_xC$ ceramics from first-principles. *Research Square*. 25 March 2020, PREPRINT. https://doi.org/10.21203/rs.3.rs-19083/v1
9. Vorotilo S., Sidnov K., Mosyagin I. Yu, Khvan A.V., Levashov E.A., Patsera E.I., Abrikosov I.A. *Ab-initio* modeling and experimental investigation of properties of ultra-high temperature solid solutions $Ta_xZr_{1-x}C$. *Journal of Alloys and Compounds*. 2019;778:480–486. https://doi.org/10.1016/j.jallcom.2018.11.219
10. Kurbatkina V.V., Patsera E.I., Levashov E.A., Vorotylo S.A., Timofeev A.N. Impact of mechanical activation pattern and conditions on carbide formation in Ta–Zr–C SHS system. *Powder Metallurgy and Functional Coatings*. 2016;(2):30–40. (In Russ.). https://doi.org/10.17073/1997-308X-2016-2-30-40

    Курбаткина В.В., Пацера Е.И., Левашов Е.А., Воротыло С.А., Тимофеев А.Н. Влияние схемы и условий механического активирования на карбидообразование в СВС-системе Ta–Zr–C. *Известия вузов. Порошковая металлургия и функциональные покрытия*. 2016;2:30–40. https://doi.org/10.17073/1997-308X-2016-2-30-40
11. Kurbatkina V.V., Patsera E.I., Vorotilo S., Levashov E.A., Timofeev A.N. Conditions for fabricating single-phase (Ta,Zr)C carbide by SHS from mechanically activated reaction mixtures. *Ceramic International Journal*. 2016;42(15):16491–16498. https://doi.org/10.1016/j.ceramint.2016.06.207
12. Patsera E.I., Levashov E.A., Kurbatkina V.V., Kovalev D.Yu. Production of ultra-high temperature carbide (Ta,Zr)C by self-propagating high-temperature synthesis of mechanically activated mixtures. *Ceramic International Journal*. 2015;41(7):8885–8893. https://doi.org/10.1016/j.ceramint.2015.03.146

13. Demirskyi D., Nishimura T., Suzuki T.S., Yoshimi K., Vasylkiv O. Consolidation and high-temperature properties of ceramics in the TaC–NbC system. *Journal of the American Ceramic Society*. 2022;105:7567–7581. https://doi.org/10.1111/jace.18660

14. Demirskyi D., Suzuki T.S., Yoshimi K., Vasylkiv O. Synthesis and high-temperature properties of medium-entropy (Ti,Ta,Zr,Nb)C using the spark plasma consolidation of carbide powders. *Open Ceramics*. 2020;2:100015. https://doi.org/10.1016/J.OCERAM.2020.100015

15. Demirskyi D., Borodianska H., Suzuki T.S., Sakka Y., Yoshimi K., Vasylkiv O. High-temperature flexural strength performance of ternary high-entropy carbide consolidated via spark plasma sintering of TaC, ZrC and NbC. *Scripta Materialia*. 2019;164:2–16. https://doi.org/10.1016/J.SCRIPTAMAT.2019.01.024

16. Stacy J., Hilmas G., Watts J., Taylor B., Rosales J. Spark plasma sintering of (Zr,Nb)C ceramics. *Journal of Alloys and Compounds*. 2025;1013:178630. https://doi.org/10.1016/j.jallcom.2025.178630

17. Wang X.G., Liu J.X., Kan Y.M., Zhang G.J. Effect of solid solution formation on densification of hot-pressed ZrC ceramics with MC (M = V, Nb, and Ta) additions. *Journal of the European Ceramic Society*. 2012;32:1795–1802. https://doi.org/10.1016/J.JEURCERAMSOC.2011.10.045

18. Orrù R., Cao G. Comparison of reactive and non-reactive spark plasma sintering routes for the fabrication of monolithic and composite ultra high temperature ceramics (UHTC) materials. *Materials*. 2013;6(5):1566–1583. https://doi.org/10.3390/ma6051566

19. Shcherbakov V.A., Gryadunov A.N., Vadchenko S.G., Alymov M.I. Exothermic synthesis and consolidation of single-phase ultra-high temperature composite Ta_4ZrC_5. *Doklady Chemistry*. 2019;488(1):242–245. https://doi.org/10.1134/S0012500819090027

Щербаков В.А., Грядунов А.Н., Вадченко С.Г., Алымов М.И. Экзотермический синтез и консолидация однофазного ультратугоплавкого композита Ta_4ZrC_5. *Доклады РАН*. 2019;488(2):153–156. https://doi.org/10.31857/S0869-56524882153-156

20. Vadchenko S.G. Induction period of a thermal explosion in titanium and aluminum powder mixtures. *Combustion, Explosion, and Shock Waves*. 2023;59(4):447–456. https://doi.org/10.1134/S001050822304007X

Вадченко С.Г. Период индукции теплового взрыва в смесях порошков титана и алюминия. *Физика горения и взрыва*. 2023;(4):60–70.

21. Vadchenko S.G., Shchukin A.S., Sytschev A.E., Boyarchenko O.D. Peculiarities of structure formation in Ni–C, Al–C, and Ni–Al–C systems at high-temperature heating. *Inorganic Materials: Applied Research*. 2022;13(1):1–6. https://doi.org/10.1134/S2075113322010385

22. Okamoto H. Desk Edition: Phase diagram for binary alloys. 2nd ed. ASM International. 900 p.

23. Lyakishev N.P. Constitution Diagrams of Binary Metallic Systems. In 3 vols. Vol. 3, book 2. Moscow: Mashinostroenie, 2000. 448 p. (In Russ.).

Диаграммы состояния двойных металлических систем: Справочник. В 3 т. Т. 3, кн. 2. Под общ. ред. Н.П. Лякишева. М: Машиностроение, 2000. 448 с.

24. Aristova N.M., Belov G.V. Thermodynamic properties of $ZrC_{0.95–0.99}$ zirconium carbide in a condensed state. *Teplofizika vysokikh temperatur*. 2022;60(1):23–32. (In Russ.). https://doi.org/10.31857/S004036442201001X

Аристова Н.М., Белов Г.В. Термодинамические свойства карбида циркония $ZrC_{0.95–0.99}$ в конденсированном состоянии. *Теплофизика высоких температур*. 2022;60(1):23–32. https://doi.org/10.31857/S004036442201001X

25. Shiryaev A. Program for thermodynamics equilibrium calculations “Thermo”. http://www.ism.ac.ru/thermo

26. Vadchenko S.G., Grigoriev Yu.M., Merzhanov A.G. Study of the ignition and combustion mechanism of Ti + C, Zr + C systems by the electrothermographic method. *Fizika goreniya i vzryva*. 1976;12(5):676–682. (In Russ.).

Вадченко С.Г., Григорьев Ю.М., Мержанов А.Г. Исследование механизма воспламенения и горения систем Ti + C, Zr + C электротермографическим методом. *Физика горения и взрыва*. 1976;12(5):676–682.

Information about the Authors

Sergei G. Vadchenko – Cand. Sci. (Phys.-Math.), Leading Researcher, Microheterogenic Process Dynamics Laboratoty, Merzhanov Institute of Structural Macrokinetics and Materials Science of the Russian Academy of Sciences (ISMAN)
ORCID: 0000-0002-2360-2114
E-mail: vadchenko@ism.ac.ru

Aleksander S. Rogachev – Dr. Sci. (Phys.-Math.), Professor, Senior Researcher, Head of the Microheterogenic Process Dynamics Laboratoty, ISMAN
ORCID: 0000-0003-1554-0803
E-mail: rogachev@ism.ac.ru

Mikhail I. Alymov – Dr. Sci. (Eng.), Professor, Corresponding Member of Russian Academy of Sciences, Director of ISMAN
ORCID: 0000-0001-6147-5753
E-mail: director@ism.ac.ru

Сведения об авторах

Сергей Георгиевич Вадченко – к.ф.-м.н., вед. науч. сотрудник лаборатории динамики микрогетерогенных процессов, Институт структурной макрокинетики и проблем материаловедения им. А.Г. Мержанова Российской академии наук (ИСМАН)
ORCID: 0000-0002-2360-2114
E-mail: vadchenko@ism.ac.ru

Александр Сергеевич Рогачев – д.ф.-м.н., гл. науч. сотрудник, профессор, зав. лабораторией динамики микрогетерогенных процессов, ИСМАН
ORCID: 0000-0003-1554-0803
E-mail: rogachev@ism.ac.ru

Михаил Иванович Алымов – д.т.н., профессор, чл. корр. РАН, директор ИСМАН
ORCID: 0000-0001-6147-5753
E-mail: director@ism.ac.ru

Contribution of the Authors

S. G. Vadchenko – preparation and conduct of the experiment, preparing the text, formulating conclusions.
A. S. Rogachev – scientific guidance, the formation of the main concept, text correction, correction of conclusions.
M. I. Alymov – setting the goal and objectives of the study, text correction, correction of conclusions.

Вклад авторов

С. Г. Вадченко – подготовка и проведение эксперимента, подготовка текста, формулировка выводов.
А. С. Рогачев – научное руководство, формирование основной концепции, корректировка текста, корректировка выводов.
М. И. Алымов – постановка цели и задачи исследования, корректировка текста, корректировка выводов.

Received 15.05.2025
Revised 16.06.2025
Accepted 20.06.2025

Статья поступила 15.05.2025 г.
Доработана 16.06.2025 г.
Принята к публикации 20.06.2025 г.